

René Meys
Laboratoire de Radioélectricité,
Université Libre de Bruxelles
B-1050 BRUSSELS, Belgium

Michel Milecan
Etudes Techniques et Constructions
Aérospace (ETCA)
PB 97, B-6000 CHARLEROI, Belgium

A B S T R A C T

Rapid advances in GaAs FET technology have raised the problem of accurately determining the noise performance of rather low gain devices at increasing frequencies. We propose a solution based on the description of noise through correlated waves that avoids many difficulties associated with classical methods (source mismatch error, biased optimum, unpredictable tuner losses, no consistency checks). It lends itself to both automation and computer implementation.

1. Introduction

It has been shown in ¹ that the noise of a linear two-port can be represented by two correlated noise sources A_n , B_n (Fig. 1). Using the levels of these sources and the correlation between them as fundamental parameters, the noise temperature of the two-port is given by :

$$T_n = \frac{T_a + |S|^2 T_b + 2 T_c |S| \cos(\Phi_s + \Phi_c)}{1 - |S|^2} \quad (1)$$

$$\text{where } T_a = \frac{|A_n|^2}{k\Delta f}, \quad T_b = \frac{|B_n|^2}{k\Delta f}, \quad T_c e^{j\Phi_c} = \frac{A_n^* B_n}{k\Delta f}$$

and $S = |S| e^{j\Phi_s}$ is the source reflection factor.

2. Outline of the method

2.1 Finding the noise temperature of a two-port

To define T_n , four parameters have to be known: T_a , T_b , T_c , Φ_c . They are found in two steps:

- A noise temperature measurement with matched source yields $T_n = T_a$, as follows from (1) with $S = 0$
- A reactive element is added to the source, that increases S to a significant value. A line stretcher is also inserted. By these means the noise temperature is measured along circle C (Fig. 2a).

From the ensuing curve (Fig. 2b), T_b , T_c , Φ_c are deduced.

2.2 Correcting for the second stage effect

The noise parameter T_a for a cascade is related to the parameters of the first ('') and second stages ('") by :

$$T_a = T'a + |T'ab|^2 T_a'' + |T'aa|^2 T_b'' - 2 \operatorname{Re}(T'ab T_a'' T_b'' e^{j\Phi_c''}) \quad (2)$$

There are similar formulas for T_b , T_c , Φ_c ². The $T'ij$'s are the wave transmission parameters of the first stage. In practice, they are derived from S_{ij} measurements.

2.3 Computing the classical noise parameters

Formulas relating the wave parameters to the classical ones are given in ¹. From them, the minimum noise temperature T_{nm} or minimum noise figure N_{fm} , together with the optimum source reflection factor S_{opt} , are readily computed.

3. How accuracy is improved

3.1 Source mismatch

As any real source has a residual reflection factor, the noise temperature measured when directly connecting it to the UUT somewhat differs from $T_n (0) = T_a$. However, for small S , equation (1) becomes :

$$T_n \approx T_a + 2 T_c |S| \cos(\Phi_s + \Phi_c) \quad (3)$$

Thus, the mean value of T_n for a 2π increase in Φ_s will be virtually equal to T_a . Accordingly, the solution is to also include the line stretcher when measuring with the "matched" source.

Fig. 3 shows an example of experimental results pertaining to a bipolar transistor at 1200 MHz. By averaging, a possible error of ± 0.10 dB on the noise figure is avoided.

3.2 An unbiased optimum

Noise measurements on components are often performed by adjusting an input tuner for minimum noise.

The corresponding reflection factor is assumed to be S_{opt} . This is only partly true because, fundamentally, S_{opt} for the device alone differs from the overall S_{opt} .

Table I contains typical differences encountered when measuring a test jig fitted with a GAT-6 FET at 18 GHz. In other cases, the second stage contribution is indeed accounted for but usually approximately. This problem is eliminated as equation (2) and similars are entirely rigorous.

3.3 The problem of losses

Losses between the noise source and UUT directly influence the noise figure. They become especially important when there is a high SWR. For good accuracy, they must be carefully evaluated. This may be a rather annoying problem with tuners, because they have two interacting settings ³. In the present case, on the contrary, a fixed reactive element is used and only one critical loss measurement has to be performed. The losses of the line stretcher are easily determined under matched conditions. A simple calculation yields their value in the unmatched working conditions.

3.4 Consistency checks

Several consistency checks are available when applying the method. If very gross faults remain in the system, one can obtain for example $T_{ba} < 0$, or the correlation coefficient

$$k = \frac{|\overline{A_n}^* \overline{B_n}|}{\sqrt{|\overline{A_n}|^2 |\overline{B_n}|^2}} = \frac{T_c}{\sqrt{T_a T_b}}$$

will fall out of the allowed range $0 \leq k \leq 1$.

An efficient accuracy test is illustrated in Fig. 4, where a test jig containing a GaAs FET is cascaded with an adapter and a post amplifier. The cascade was divided into a first and second stage at points B or B'.

Table II summarizes the noise parameters at 18 GHz for a) the cascade AC, b) second stage BC, c) second stage B'C, d) first stage AB, e) first stage AB'.

These last are very similar, though the intermediate results are strongly different.

A closer agreement was even found when the effect of the adapter was removed (case f).

As long as a significant error cause remains in either the noise parameters or the first stage S parameters such an agreement does not occur.

Conversely, once it has been reached, confidence is permitted.

4. Supplementary features

4.1 De-embedding

Due to the analytical nature of its mathematics, the noise waves method also offers easy de-embedding of components from their test jig.

4.2 Possibility of automation

Recent work has shown that the method lends itself to fully automatic and complete noise characterization.

For this purpose, the line stretcher is replaced by a "long" section of air line. It is now possible to move around circle C in Fig. 2 by slightly changing the frequency, say by 1%.

Over such small an interval the noise parameters of most devices remain almost constant and the procedure is equivalent to extending the line-stretcher at a fixed frequency.

4.3 Computer implementation

Of course, the practical application of the steps outlined in section 2 will be most easily achieved when a computer program is at hand. Such a program has been written at ETCA. Run time on a desktop computer does not exceed a few seconds since no iterations are required.

5. Conclusions

Using the concept of noise waves as a guideline led to an entirely new approach to noise problems.

Extended experimental work on bipolar transistors in the lower microwave range and GaAs FET's

in Ka-band made evident the many associated advantages.

When both automation and computer aided implementation are added, a very efficient tool for analyzing the noise behaviour of microwave devices can result. Such a system is presently under development in the 27 to 30 GHz frequency range under an European Space Agency contract for installation at the ESTEC facilities. Let us finally mention that present work indicates that the noise waves method could introduce an improved solution to the challenging problem of fast and accurate ENR calibration.

6. Acknowledgments

We thank the TRC department of ESTEC for having supported part of this work under ESA contract number 4172/79/NL/DG.

7. References

- (1) R.P. Meys, "A Wave Approach to the Noise Properties of Linear Microwave Devices", IEEE Transactions on Microwave Theory and Techniques, Vol. MTT-26, pp.34-37, January 1978.
- (2) R. Meys and M. Milecan, "A computer Based Method Giving the Experimental Noise Parameters of Q-ports through the Use of New Noise Sources", Proceedings of SPACECAD 79, ESA SP-146, pp.387-396, November 1979.
- (3) E.W. Strid, "Measurement of Losses in Noise-Matching Networks", IEEE Transactions on Microwave Theory and Techniques, Vol. MTT-29, pp. 247-252, March 1981

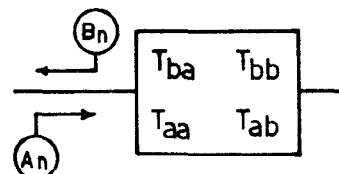


Fig. 1 The model for a linear noisy two-port

	Mod(S _{opt})	Arg (S _{opt}) DEG
Overall	.472	88
First Stage	.440	72

Table I. Experimental differences between the optimum source reflection factor for the overall chain and its first stage.

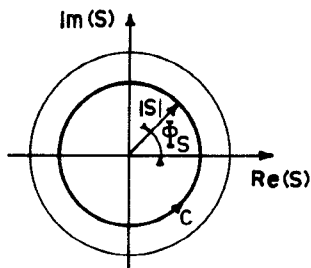
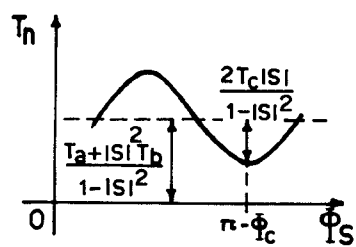
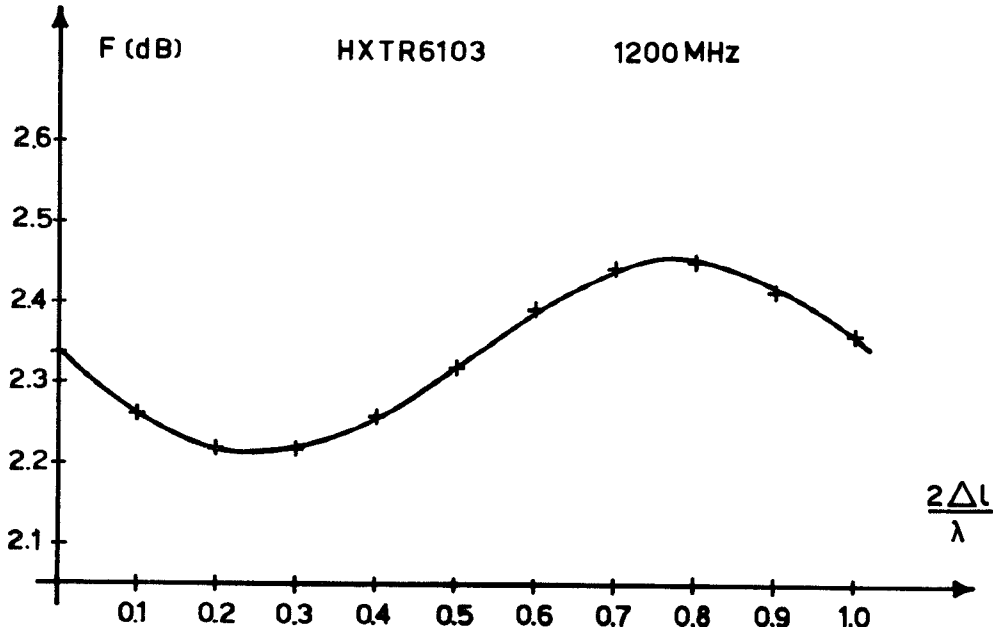


Fig. 2



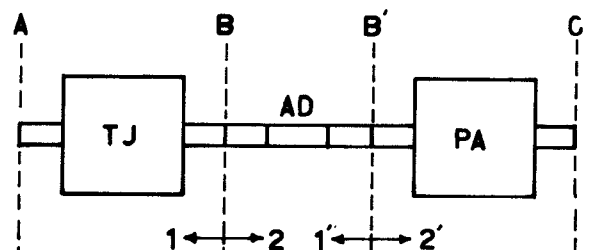
a) Circle C in the S plane along which the noise temperature T_n is measured

b) The corresponding variation of T_n



The variation of the noise figure due to the residual source reflection factor as a function of the normalized line-stretcher extension

Fig. 3



Several ways for dividing a cascade into first and second stages.

Fig. 4

Two-port	T_a (K)	T_b (K)	T_c (K)	Φ_c (DEG)	T_{nm} (K)	NF_m (dB)	$Mod_{(S_{opt})}$	$Arg(S_{opt})$ (DEG)
a) AC	1747	630	918	92				
b) BC	1852	996	1295	-179				
c) B'C	868	248	80	-119				
d) AB	794	335	417	108	610	4.92	.440	72
e) AB'	855	362	452	105	654	5.13	.445	75
f) AB	842	358	445	106	644	5.08	.445	74

TABLE II. The noise parameters for the two-ports shown in Fig. 4. For convenience, the classical parameters T_{nm} and S_{opt} are also given.